Liquid Crystals
Publication details, including instructions for authors and subscription information:
http://www.informaworld.com/smpp/title~content=t713926090

Synthesis and properties of phenyl benzoate-based and biphenyl-based liquid crystalline thiol-ene monomers

H. T. A. Wilderbeek[a]; M. G. M. van der Meer[a]; M. A. G. Jansen[b]; L. Nelissen[b]; H. R. Fischer[c]; J. J. G. S. van Es[b]; C. W. M. Bastiaansen; J. Lub[d]; D. J. Broer
[a] Dutch Polymer Institute, P.O. Box 902, 5600 AX Eindhoven, The Netherlands, [b] Eindhoven University of Technology, P.O. Box 513, 5600 MB Eindhoven, The Netherlands, [c] TNO TPD, De Rondom 1, 5612 AP Eindhoven, The Netherlands, [d] Philips Research Laboratories, Professor Holstlaan 4, 5656 AA Eindhoven, The Netherlands,

Online publication date: 11 November 2010

To cite this Article Wilderbeek, H. T. A. , van der Meer, M. G. M. , Jansen, M. A. G. , Nelissen, L. , Fischer, H. R. , van Es, J. J. G. S. , Bastiaansen, C. W. M. , Lub, J. and Broer, D. J.(2003) 'Synthesis and properties of phenyl benzoate-based and biphenyl-based liquid crystalline thiol-ene monomers', Liquid Crystals, 30: 1, 93 — 108
To link to this Article: DOI: 10.1080/0267829021000001746
URL: http://dx.doi.org/10.1080/0267829021000001746

LIQUID CRYSTALS, 2003, VOL. 30, NO. 1, 93–108

Synthesis and properties of phenyl benzoate-based and biphenyl-based liquid crystalline thiol-ene monomers

H. T. A. WILDERBEEK*†‡, M. G. M. VAN DER MEER‡§, M. A. G. JANSEN‡, L. NELISSEN‡, H. R. FISCHER¶, J. J. G. S. VAN ES‡, C. W. M. BASTIAANSEN†‡, J. LUB§ and D. J. BROER‡§

†Dutch Polymer Institute, P.O. Box 902, 5600 AX Eindhoven, The Netherlands
‡Eindhoven University of Technology, P.O. Box 513, 5600 MB Eindhoven, The Netherlands
§Philips Research Laboratories, Professor Holstlaan 4, 5656 AA Eindhoven, The Netherlands
¶TNO TPD, De Rondom 1, 5612 AP Eindhoven, The Netherlands

(*Received 30 May 2002; in final form 12 August 2002; accepted 18 September 2002*)

Novel phenyl benzoate-based and biphenyl-based liquid crystalline thiol-ene monomers were synthesized and their properties investigated. By varying the bridging unit and spacer length, the type of mesophase can be tuned from the low ordered nematic and smectic A phase in the case of the phenyl benzoate-based monomers, to the highly ordered crystal E phase for the biphenyl-based monomers and their corresponding bromo precursors. We investigated the degree of order of the phenyl benzoate-based materials using the Haller method. Possible premature polymerization of these monomers was examined by size exclusion chromatography. The materials exhibit low transition temperatures and a high stability at typical handling times and temperatures. Consequently, these monomers are useful for *in situ* polymerization with anisotropic inert solvents, which could potentially lead to new architectures and enhanced electro-optical properties of devices. The use of the biphenyl-based monomers appears to be of limited use for polymerizations in anisotropic solution. However, as a result of their intrinsic high degree of molecular order, these monomers form a particularly interesting class of reactive materials that can be bulk polymerized to give main chain polymers with highly defined mechanical and optical or electro-optical properties.

1. Introduction

In the pursuit of increased efficiency and functionality, polymer stabilized liquid crystal effects have been investigated as a means of further optimizing liquid crystal-based devices. In particular, combinations of low molecular mass liquid crystals and either flexible polymers [1], dispersed polymer particles [2], side group liquid crystal polymers [3], and isotropic or anisotropic network-type structures [4–6] have been considered. However, the order parameter of the mesogenic moieties in conventional side group or network-type systems is comparable to the order parameter of low molar mass LCs, and is limited to a maximum of about 0.7. Although rotational mobility is hindered, a higher order parameter should be possible in principle, but is limited by the steric hindrance caused by the polymer backbone. This hinders perfect alignment of the core, despite the decoupling of the mesogenic core from the polymer backbone.

*Author for correspondence;
e-mail: hans.wilderbeek@philips.com

In the case of main chain polymers, it is anticipated that the whole molecule is aligned to a high degree of order, resulting from the larger aspect ratio [7, 8], thus giving rise to a higher degree of orientation in comparison with the side group and network-type structures. Consequently, an enhanced optical performance (e.g. contrast ratio, faster relaxation) can be realized, potentially leading to fast nematic switches, stabilized ferroelectrics or switchable gratings, for instance, depending on the actual morphology of the polymer/LC composite on a nanoscale or microscale.

Until now, the only reported structures similar to the main chain polymer/LC systems are based on reversible, non-covalently linked building blocks dispersed in anisotropic solvents [9–11]. However, the polymerization process that involves generation of covalent bonds has a significant advantage over the reversible non-covalent structures: it can be initiated on demand at a fixed temperature through the use of UV-irradiation. This also introduces the possibility of the formation of the polymeric structures at specified positions, for example

Liquid Crystals ISSN 0267-8292 print/ISSN 1366-5855 online © 2003 Taylor & Francis Ltd
http://www.tandf.co.uk/journals
DOI: 10.1080/0267829021000001746

through patterning processes or holographic approaches, thus further extending the control over the final morphology.

To create the proposed covalently linked systems, materials must be available that enable the generation of such linear polymeric architectures. Thiol-ene monomers can be polymerized through a free-radical propagated step-growth mechanism [12] leading to the desired main chain polymers. In addition, monomers containing a thiol functionality benefit, for instance, from having specific thiol–substrate interactions which provide additional means of morphology control through the patterned alignment of liquid crystals [13]. Liquid crystalline thiol-ene monomers have been reported before [7], but their use was directed towards bulk polymerization. Here, we have designed novel polymer/LC systems based on the *in situ* polymerization of an initially homogeneous mixture of a mesogenic thiol-ene monomer and an inert anisotropic solvent. In order to generate homogeneous mixtures of monomer and solvent at ambient temperatures, liquid crystalline thiol-ene monomers with low melting temperatures are required. Yet, the reported liquid crystalline thiol-ene monomers display high transition temperatures originating from their bulky rigid triple phenyl core, despite the attempt to lower the transitions by introducing asymmetry through a methyl substituent. A single compound with a smaller mesogenic group based on a double phenyl core was shown to exhibit lower temperatures [7] and therefore forms an ideal template for further synthesis of other homologues.

Control over the resulting morphology is obviously of vital importance. The intended systems are formed *in situ* from initially homogeneous mixtures of liquid crystalline monomers and inert liquid crystalline solvents, such as the familiar cyanobiphenyl derivatives. During the course of this polymerization, phase separation of the forming oligomers/polymers will occur. Consequently, the onset of phase separation, whether it occurs early or later in the polymerization process, is an important parameter in the realization of the ultimate morphology and the associated electro-optical properties of the system. However, the chemical structure of the above mentioned double phenyl core-based thiol-ene monomers differs significantly from the chemical structure of the cyanobiphenyls used for the anisotropic solvent. The modification of the chemical structure of the thiol-ene monomer so that it resembles that of the inert anisotropic solvent used, i.e. the cyanobiphenyl, offers an additional tool for further tuning of the morphological development by influencing the onset of phase separation.

In this paper we describe the synthesis and properties of novel phenyl benzoate-based and biphenyl-based liquid crystalline thiol-ene derivatives. We also describe initial investigations into the mixing behaviour of the biphenyl-based monomers with cyanobiphenyl solvents, aimed at the subsequent *in situ* polymerization of the thiol-ene monomers. The thiol and vinyl group are both incorporated within these monomers, ensuring the optical theoretically required 1 : 1 thiol–olefin stoichiometry at all times.

2. Experimental

2.1. *Materials*

Hydrochloric acid, diethyl ether, ethanol, dichloromethane, 2-butanone, sodium chloride, lithium aluminium hydride, 5-hexen-1-ol, hydroquinone, 1,4-dibromobutane, 1,5-dibromopentane, 1,6-dibromohexane and sodium hydroxide pellets were supplied by Merck (Merck, Darmstadt, Germany or Merck-Schuchardt, Hohenbrunn, Germany). All other chemicals were supplied by Acros Organics (Geel, Belgium), with the exception of magnesium sulphate, tetrabutylammonium bromide (Fluka Chemical, Buchs, Switzerland), 3-buten-1-ol, sulphur, acetic acid (Sigma Aldrich Co., Steinheim, Germany) and the photoinitiator Irgacure 651 (α,α-dimethoxydeoxybenzoin; Ciba Specialty Chemicals, Basel, Switzerland).

Fischer Scientific ('s-Hertogenbosch, The Netherlands) supplied petroleum ether (40–65°C and 60–80°C). The petroleum ether was distilled before use according to standard procedures [14]. The pre-run of the distillation was discarded. The tetrahydrofuran used for the Grignard syntheses was rigorously dried using lithium aluminium hydride, following the procedure described elsewhere [14].

All chemicals and solvents were of the p.a. grade or of at least comparable purities, and were used without further purification unless stated otherwise.

2.2. *Characterization*

FTNMR spectra were recorded using a Varian 400 MHz spectrometer at the resonance frequencies of 400.162 MHz for ^{1}H-resonance spectra and 100.630 MHz for ^{13}C-resonance spectra. All spectra were recorded using $CDCl_3$ as solvent at 25°C. All chemical shifts are reported in ppm downfield from tetramethylsilane (TMS), used as an internal standard ($\delta = 0$ ppm). The coupling constants J are given in Hz. The assignment of the chemical shifts was further evaluated using gCOSY or HETCOR experiments where necessary. Elemental analysis was performed using a Perkin Elmer CHN analyser type 2400. Mass spectra were determined using a Shimadzu GC-MS QP5000 mass spectrometer. Refractive indices were determined using an Abbé refractometer (Atago 2T and 4T). Thermal characterization was performed using a Perkin-Elmer DSC-7 Differential Scanning Calorimeter (DSC) or Pyris1 DSC together with a CCA-7 temperature controller at standard heating rates ranging from 2 to 10°C min^{-1}. The DSCs were calibrated using indium, zinc, hexatriacontane, *n*-octane

and *n*-dodecane standards of high purity. Transition enthalpies and entropies were determined from specific heat capacity measurements following procedures described elsewhere [15]. Care was taken that the mass of the aluminium sample pan was as close as possible to that of the reference pan. Transition temperatures were determined and texture micrographs were obtained using a Zeiss MC63 microscope with polarization optics in combination with a Linkam THMS600 hot stage. The samples were observed at heating rates not exceeding $1^{\circ}C\,min^{-1}$ close to the actual transitions in order to determine the actual transition temperature.

Size exclusion chromatography (SEC) was performed using a Waters type 710B injector (50 µl) and two Polymer Labs, mixed-d, 7.8 × 300 mm columns thermostated by a Spark Holland Mistral thermostat at 30°C. A Waters type 6000 pump provided a constant flow of $1\,ml\,min^{-1}$ of chloroform. A Waters model 440 UV-detector ($\lambda = 254$ nm and $\lambda = 263$ nm) was used for detection.

FTIR spectra were recorded using a Mattson Polaris FTIR spectrometer at a resolution of $2\,cm^{-1}$. Wide angle X-ray scattering (WAXS) experiments were perfomed using a Siemens 2D multi-wire area detector X1000 filled with Xe-methane. A Cu-K_{α} wavelength of 1.542 Å was used in combination with a flat graphite monochromator, collimated to 0.6 mm. Sample temperatures were controlled using a Linkam THMS600 hot stage. WAXS experiments were also performed at the European Synchrotron Radiation Facility (ESRF), Grenoble, France. The radiation source provided monochromatic X-rays of wavelength 0.71795 Å. Each diffraction pattern was recorded for 2 to 5 s on a two-dimensional Princeton CCD detector. Two-dimensional X-ray patterns were transformed into one-dimensional patterns using a FIT2D programme (ESRF), by performing integration along the azimuthal angle.

2.3. *Synthesis*

The following materials were prepared according to previously described procedures: ethyl 4-(6-bromohexyloxy)benzoate (**BrA 6**) [7], ethyl 4-(5-bromopentyloxy)benzoate (**BrA 5**) [8], 4-(6-mercaptohexyloxy)benzoic acid (**ThA 6**) [7], 4-(5-mercaptopentyloxy)benzoic acid (**ThA 5**) [8], and 3-buten-1-yl *p*-toluenesulphonate (**TsE 4**) [16]. More details regarding these procedures and those described below can be found elsewhere [17].

2.3.1. *Ethyl 4-(4-bromobutyloxy)benzoate (**BrA 4**)*

This compound was prepared in 43% yield after fractionation (b.p. = 157°C at 0.055 mbar) by a procedure similar to one described for **BrA 6** [7], starting from 1,4-dibromobutane. The product showed traces of an olefinic impurity. Despite recrystallization experiments, no improvements in purity could be achieved. ^{1}H NMR ($CDCl_3$, 25°C, 400.134 MHz): 8.03 (d, 2H, $^3J = 9.0$, C<u>H</u> pos.2), 6.92 (d, 2H, $^3J = 9.0$, C<u>H</u> pos.3), 4.36 (q, 2H, $^3J = 7.1$, C<u>H</u>$_2$–CH_3), 4.08 (t, 2H, $^3J = 6.5$, C<u>H</u>$_2$–O–Ph), 3.51 (t, 2H, $^3J = 6.9$, C<u>H</u>$_2$–Br), 2.08 + 1.98 (2m, 4H, Br–CH_2–(C<u>H</u>$_2$)$_2$–CH_2), 1.43 (t, 3H, $^3J = 7.2$, C<u>H</u>$_3$). ^{13}C NMR ($CDCl_3$, 25°C, 100.614 MHz): 166.4 (<u>C</u>OO–CH_2), 162.5 (<u>C</u> pos.1), 131.5 (<u>C</u> pos.3), 123.0 (<u>C</u> pos.4), 113.9 (<u>C</u> pos.2), 67.0 (<u>C</u>–O–Ph), 60.6 (<u>C</u>–CH_3), 33.3 + 29.3 + 27.7 (Br–(<u>C</u>H_2)$_3$–CH_2–O).

2.3.2. *4-(4-Mercaptobutyloxy)benzoic acid (**ThA 4**)*

Using a slightly modified procedure to that reported for the synthesis of 4-(6-mercaptohexyloxy)benzoic acid (**ThA 6**) [7], 85.0 g (282 mmol) of ethyl 4-(4-bromobutyloxy)benzoate **BrA 4**, 55 ml of water and 32.4 g (426 mmol) of thiourea were used. The initially inhomogeneous mixture was heated for 2 h at 110°C, during which time the mixture slowly became transparent. Over a period of 25 min, 80 ml of freshly distilled toluene were carefully added to the boiling mixture, while vigorously stirring. The isothiuronium salt was allowed to crystallize when the mixture was cooled to room temperature. The salt was filtered off and washed with toluene to remove completely the olefinic by-products from the synthesis of **BrA 4**. 360 ml of 10% sodium hydroxide solution were added to the purified salt and the mixture was heated at reflux for 2 h. The hot solution was transferred to a 3-litre beaker while vigorously stirring. A 2.5M hydrochloric acid solution was slowly added until the pH was 1. The precipitate was filtered off and the residue was washed twice using 400 ml of water (until pH = 4–5). The white solid obtained in this way was dried under vacuum at 55 to 60°C. The yield after recrystallization from petroleum ether (60–80°C)/2-butanone was 23.2 g (36%); no olefinic signals were observed by NMR. Transitions (°C): Cr 118.8 N 139.4 I. ^{1}H NMR ($CDCl_3$, 25°C, 400.134 MHz): 8.06 (d, 2H, $^3J = 9.0$; $^nJ = 2.1$, C–<u>H</u> pos.2), 6.93 (d, 2H, $^3J = 8.9$; $^nJ = 2.0$, C–<u>H</u> pos.3), 4.07 (t, 2H, $^3J = 6.4$, C<u>H</u>$_2$–O–Ph), 2.63 (d-t, 2H, $^3J = 7.7$; $^3J = 7.1$, C<u>H</u>$_2$–SH), 1.94 (m, 2H, C<u>H</u>$_2$–CH_2–O), 1.84 (m, 2H, C<u>H</u>$_2$–CH_2–SH), 1.40 (t, 1H, $^3J = 7.7$, S<u>H</u>), COO<u>H</u> not observed. ^{13}C NMR ($CDCl_3$, 25°C, 100.614 MHz): 171.0 (<u>C</u>OOH), 162.4 (<u>C</u> pos.4), 132.7 (<u>C</u> pos.2), 121.6 (<u>C</u> pos.1), 114.6 (<u>C</u> pos.3), 68.3 (<u>C</u>–O–Ph), 31.2 (<u>C</u>–CH_2–SH), 28.4 (<u>C</u>–CH_2–O), 25.1 (<u>C</u>–SH).

2.3.3. *5-Hexen-1-yl p-toluenesulphonate (**TsE 6**)*

This compound was prepared in 97% yield by a procedure similar to one described for 3-buten-1-yl *p*-toluenesulphonate (**TsE 4**) [16], starting from 5-hexen-1-ol. ^{1}H NMR ($CDCl_3$, 25°C, 400.134 MHz):

7.79 (d, 2H, $^3J = 8.4$, C–H *meta* to C–CH_3), 7.35 (d, 2H, $^3J = 8.4$, C–H *ortho* to C–CH_3), 5.72 (m, 1H, $^3J = 6.5$; $^3J = 16.9$; $^3J = 10.1$, ε-H), 4.96 (m, 1H, $^2J = 1.2$; $^3J = 16.8$, ζ-H (*cis*)), 4.93 (m, 1H, $^2J = 1.1$; $^3J = 10.0$, ζ-H (*trans*)), 4.03 (t, 2H, $^3J = 6.7$, α-H), 2.45 (s, 3H, CH_3), 2.00 + 1.65 + 1.41 (m, 6H, β-γ-δ-H). ^{13}C NMR ($CDCl_3$, 25°C, 100.614 MHz): 145.0 (C–CH_3), 138.2 (ε-C), 133.5 (C–SO_3), 130.1 (C *ortho* to C–CH_3), 128.2 (C *meta* to C–CH_3), 115.3 (ζ-C), 70.7 (α-C), 33.2 (δ-C), 28.5 (β-C), 24.8 (γ-C), 21.9 (CH_3).

2.3.4. *4-(5-Hexenyloxy)phenol (**PhE 6**)*

Using a slightly modified procedure to that reported earlier [18], 17.1 g (67.3 mmol) of 5-hexen-1-yl *p*-toluenesulphonate (**TsE 6**) was slowly added over a period of approximately 2 h to a mixture of hydroquinone (7.79 g, 70.7 mmol), sodium methoxide (3.82 g, 70.7 mmol) and 100 ml of *N*,*N*-dimethylformamide. The mixture was stirred for 24 h at 70°C. After concentration using a rotary evaporator, 200 ml of a 5M NaOH solution was added. The aqueous solution was washed with 300 ml of diethyl ether and acidified using a 5M HCl solution until the pH was 1. Subsequent extraction using two 200 ml portions of dichloromethane, washing of the dichloromethane phase with 500 ml of water, drying with magnesium sulphate and concentration of the solution resulted in 2.63 g of the red coloured phenol (22%). ^{1}H NMR ($CDCl_3$, 25°C, 400.134 MHz): 6.77 (d, 2H, $^3J = 9.0$, CH *meta* to OH), 6.73 (d, 2H, $^3J = 9.0$, CH *ortho* to OH), 5.84 (m, 1H, $^3J = 6.6$; $^3J = 17.1$; $^3J = 10.2$, ε-H), 5.04 (m, 1H, $^3J = 17.1$; $J = 1.5$, ζ-H (*trans*)), 4.98 (m, 1H, $^3J = 10.2$; $^2J = 1.5$, ζ-H (*cis*)), 3.92 (t, 2H, $^3J = 6.6$, α-H), 2.14 + 1.79 + 1.58 (3m, 6H, β,γ,δ-H). ^{13}C NMR ($CDCl_3$, 25°C, 100.614 MHz): 153.3 (C pos.4), 149.3 (C pos.1), 138.6 (ε-C), 116.0 + 115.6 (C pos.2 + pos.3), 114.7 (ζ-C), 68.5 (α-C), 33.5 (δ-C), 28.8 (β-C), 25.3 (γ-C).

2.3.5. *4-(3-Butenyloxy)phenol (**PhE 4**)*

Similar to the procedure described for the synthesis of 4-(5-hexenyloxy)phenol (**PhE 6**), 62.7 g (0.277 mol) of 3-buten-1-yl *p*-toluenesulphonate (**TsE 4**) and 61.1 g (0.555 mol) of hydroquinone were dissolved in 300–400 ml of ethanol. The mixture was heated at reflux and 60 ml of 5M sodium hydroxide was slowly added to the mixture, followed by an additional reflux period of 10–12 h. The excess of ethanol/water was removed using a rotary evaporator at diminished pressure. 24.1 g of a brown solid was obtained (53%) after purification as described for **PhE 6**. ^{1}H NMR ($CDCl_3$, 25°C, 400.134 MHz): 6.77 (d, 2H, $^3J = 8.8$, CH *meta* to OH), 6.73 (d, 2H, $^3J = 8.8$, CH *ortho* to OH), 5.87 (m, 1H, $^3J = 6.6$; $^3J = 17.2$; $^3J = 10.2$, γ-H), 5.17 (m, 1H, $^3J = 17.2$; $^2J = 1.5$, δ-H (*trans*)), 5.10 (m, 1H, $^3J = 10.2$; $^2J = 1.5$, δ-H (*cis*)), 3.95 (t, 2H, $^3J = 6.6$, α-H), 2.52 (m, 2H, $^3J = 6.6$; $^3J = 6.6$, β-H). ^{13}C NMR ($CDCl_3$, 25°C, 100.614 MHz): 153.0 (C pos.4), 149.5 (C pos.1), 134.5 (γ-C), 117.4 (δ-C), 116.5 + 116.2 (C pos.2 + pos.3), 68.1 (α-C), 33.7 (β-C).

2.3.6. *4-(5-Hexenyloxy)phenyl 4-(6-mercaptohexyloxy)-benzoate (**ThE 6b6**)*

The esterification was performed using a procedure described in [7], starting from 4-(6-mercaptohexyloxy)-benzoic acid (**ThA 6**) and 4-(5-hexenyloxy)phenol (**PhE 6**). The crude product was purified by flash column chromatography (silica) using a petroleum ether (60–80°C)/dichloromethane gradient, from 100.0 to 70/30 v/v. A white solid was obtained in 23% yield. Transitions (°C): Cr 42.5 SmA 55.4 N 69.5 I.

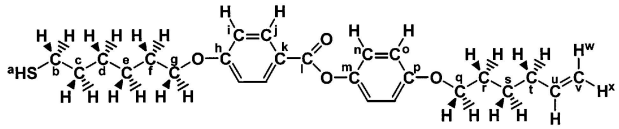

^{1}H NMR ($CDCl_3$, 25°C, 400.134 MHz): 8.13 (d, 2H, $^3J = 8.9$, H^j), 7.10 (d, 2H, $^3J = 9.1$, H^n), 6.96 (d, 2H, $^3J = 9.1$, H^i), 6.91 (d, 2H, $^3J = 9.0$, H°), 5.84 (m, 1H, $^3J_{ut} = 6.6$; $^3J_{uw} = 17.0$; $^3J_{ux} = 10.2$, H^u), 5.04 (m, 1H, $^3J_{wu} = 17.0$; $^nJ = 1.6$, H^w), 4.98 (m, 1H, $^2J = 1.4$; $^3J_{xu} = 10.2$, H^x), 4.04 (t, 2H, $^3J = 6.4$, H^g), 3.97 (t, 2H, $^3J = 6.5$, H^q), 2.56 (q, 2H, H^b), 2.13 + 1.81 + 1.66 + 1.57 + 1.49 (5m, 14H, $H^{c+d+e+f+r+s+t}$), 1.35 (t, 1H, $^3J_{ab} = 7.7$, H^a). ^{13}C NMR ($CDCl_3$, 25°C, 100.614 MHz): 163.5 (C^l), 156.9 (C^p), 144.5 (C^m), 138.7 (C^u), 132.4 (C^j), 122.6 (C^n), 121.9 (C^k), 115.2 (C^o), 114.7 (C^v), 114.4 (C^i), 68.3 + 68.2 (C^{g+q}), 34.0 (C^c), 33.6 (C^t), 29.1 (C^r), 28.9 (C^f), 28.2 (C^d), 25.7 (C^s), 25.5 (C^e), 24.7 (C^b). FTIR (KBr, 20°C, cm^{-1}): 3064 (w) + 3002 (w) (C–H str. in vinyl; aryl–H str.), 2934 (m) + 2856 (m) (C–H str. in $-CH_2-$), 2570 (w) (–S–H), 1732 (s) (C=O str.), 1609 (s) + 1580 (m) + 1512 (s) (C=C str. in aryl), 1475 (w) + 1422 (w) + 1394 (w) (C–H deform. in $-CH_2-$), 1275 (sh) + 1255 (s) + 1197 (s) + 1171 (s) (from ester funct.), 1080 (m) (not acc.), 1009 (m) + 914 (w) (R–CH=CH_2), 845 (m) (1,4-disubst. aryl). Raman (20°C, cm^{-1}): 2563 (m) (–S–H), 1726 (s) (C=O), 1640 (w) (vinyl). Found: C 70.73 (calc. 70.06%), H 7.75 (calc. 7.53%). UV-Vis ($CHCl_3$): $\lambda_{max} = 263$ nm.

2.3.7. *4-(3-Butenyloxy)phenyl 4-(6-mercaptohexyloxy)-benzoate (**ThE 6b4**)*

This synthesis was similar to one described for 4-(5-hexenyloxy)-phenyl 4-(6-mercaptohexyloxy)benzoate (**ThE 6b6**). The crude product was crystallized from ethanol at 0°C before flash column chromatographic

separation (silica, petroleum ether 40–65°C/dichloromethane = 30/70 v/v; $R_f = 0.32$). Yield: 48%, transitions (°C): Cr 53.5 (SmA 48.3) N 67.7 I.

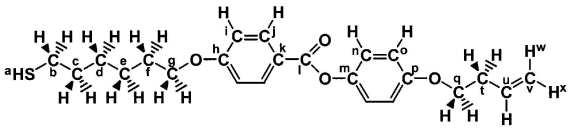

The NMR signal assignment differs from that of **ThE 6b6**, in the olefinic part. ^{1}H NMR ($CDCl_3$, 25°C, 400.134 MHz): 5.91 (m, 1H, $^3J_{ut} = 6.6$; $^3J_{uw} = 17.3$; $^3J_{ux} = 10.3$, H^u), 5.18 (m, 1H, $^2J = 1.1$; $^3J_{wu} = 17.3$; $^4J_{wt} = 1.5$, H^w), 5.12 (m, 1H, $^2J = 1.1$; $^3J_{xu} = 10.3$, H^x), 4.02 (t, 2H, $^3J = 6.6$, H^q), 2.55 (m, 4H, $^3J_{tq} = 6.6$; $^3J_{tu} = 6.6$, H^{b+t}). ^{13}C NMR ($CDCl_3$, 25°C, 100.614 MHz): 134.5 (C^u), 117.2 (C^v), 68.2 + 67.8 (C^{g+q}), 33.8 (C^t). FTIR (KBr, 20°C, cm^{-1}): 3073 (w) + 3003 (w) (C–H str. in vinyl; aryl–H str.), 2941 (m) + 2924 (m) + 2866 (sh) + 2858 (m) (C–H str. in $-CH_2-$), 2572 (w) (–S–H), 1724 (s) (C=O str.), 1609 (s) + 1581 (m) + 1512 (s) + 1505 (s) (C=C str. in aryl), 1474 (m) + 1422 (m) + 1396 (w) (C–H deform. in $-CH_2-$), 1281 (s) + 1259 (s) + 1249 (s) + 1198 (s) + 1172 (s) (from ester funct.), 1077 (s) (not acc.), 1009 (s) + 928 (m) (R–CH=CH_2), 846 (s) (1,4-disubst. aryl). Raman (20°C, cm^{-1}): 2572 (m) (–S–H), 1715 (s) (C=O), 1643 (w) (vinyl). Found: C 69.07 (calc. 68.97%), H 6.98 (calc. 7.05%). UV-Vis ($CHCl_3$): $\lambda_{max} = 263$ nm.

2.3.8. *4-(3-butenyloxy)phenyl 4-(5-mercaptopentyloxy)-benzoate (**ThE 5b4**)*

This synthesis was similar to the one described for 4-(5-hexenyloxy)-phenyl 4-(6-mercaptohexyloxy)benzoate (**ThE 6b6**). A white powder was obtained in 46% yield after flash column chromatography (petroleum ether 40–65°C/dichloromethane = 30/70 v/v; $R_f = 0.28$). Transitions (°C): Cr 60.6 N 64.2 I.

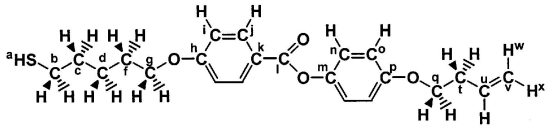

The NMR signal assignment differs from that of **ThE 6b4**, in the mercaptoalkyl part. ^{1}H NMR ($CDCl_3$, 25°C, 400.134 MHz): 4.05 (t, 2H, $^3J = 6.3$, H^g), 2.58 (d-t, 2H, $^3J_{ba} = 7.7$; $^3J_{bc} = 7.0$, H^b), 1.84 + 1.70 + 1.60 (3m, 6H, H^{c+d+f}), 1.37 (t, 1H, $^3J = 7.7$, H^a). ^{13}C NMR ($CDCl_3$, 25°C, 100.614 MHz): 68.1 + 67.8 (C^{g+q}), 33.8 (C^{c+t}), 28.7 (C^f), 25.0 (C^d), 24.6 (C^b). FTIR (KBr, 20°C, cm^{-1}): 3076 (w) + 3010 (sh) (C–H str. in vinyl; aryl–H str.), 2931 (m) + 2870 (m) (C–H str. in $-CH_2-$), 2573 (w) (–S–H), 1725 (s) (C=O str.), 1606 (s) + 1580 (m) + 1510 (s) + 1503 (s) (C=C str. in aryl), 1469 (m) + 1422 (m) + 1389 (w) (C–H deform. in $-CH_2-$), 1273 (sh) + 1255 (s) + 1195 (s) = 1170 (s) (from ester funct.), 1079 (s) (not acc.), 1010 (s) + 926 (m) (R–CH=CH_2), 846 (s) (1,4-disubst. aryl). Raman (20°C, cm^{-1}): 2570 (m) (–S–H), 1723 (s) (C=O), 1641 (w) (vinyl). Found: C 68.60 (calc. 68.37%), H 6.75 (calc. 6.78%). UV-Vis ($CHCl_3$): $\lambda_{max} = 263$ nm.

2.3.9. *4-(3-Butenyloxy)phenyl 4-(4-mercaptobutyloxy)-benzoate (**ThE 4b4**)*

This synthesis was similar to the one described for 4-(5-hexenyloxy)-phenyl (4-(6-mercaptohexyloxy)benzoate (**ThE 6b6**). A white powder was obtained in 59% yield after flash column chromatography using a petroleum ether 40–65°C/dichloromethane gradient, from 40/60 to 20/80 v/v, $R_f = 0.35$. Transitions (°C): Cr 58.6 N 68.4 I.

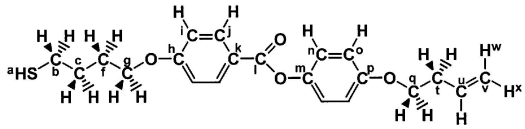

The NMR signal assignment differs from those of **ThE 5b4** and **ThE 6b4**, in the mercaptoalkyl part. ^{1}H NMR ($CDCl_3$, 25°C, 400.134 MHz): 4.07 (t, 2H, $^3J = 6.3$, H^g), 2.63 (d-t, 2H, $^3J_{ba} = 7.7$; $^3J_{bc} = 7.1$, H^b), 1.94 (m, 2H, H^f), 1.84 (m, 2H, H^c), 1.40 (t, 1H, $^3J = 7.7$, H^a). ^{13}C NMR ($CDCl_3$, 25°C, 100.614 MHz): 68.3 + 68.2 (C^{g+q}), 31.2 (C^c), 28.5 (C^f), 25.1 (C^b). FTIR (KBr, 20°C, cm^{-1}): 3059 (w) + 3012 (w) (C–H str. in vinyl; aryl–H str.), 2951 (m) + 2936 (m) + 2925 (m) + 2870 (m) + 2853 (m) (C–H str. in $-CH_2-$), 2573 (w) (–S–H), 1724 (s) (C=O str.), 1607 (s) + 1580 (m) + 1512 (s) (C=C str. in aryl), 1472 (m) + 1448 (w) + 1424 (m) + 1389 (w) (C–H deform. in $-CH_2-$), 1283 (s) + 1252 (s) + 1197 (s) + 1171 (s) (from ester funct.), 1075 (s) (not acc.), 1009 (s) + 924 (m) (R–CH=CH_2), 846 (s) (1,4-disubst. aryl). Raman (20°C, cm^{-1}): 2573 (m) (–S–H), 1718 (s) (C=O), 1641 (w) (vinyl). Found: C 67.85 (calc. 67.72%), H 6.49% (calc. 6.49%). UV-Vis ($CHCl_3$): $\lambda_{max} = 263$ nm.

2.3.10. *Synthesis of 4-bromo-4′-(5-hexenyloxy)biphenyl (**BrE 0.6**)*

Over a period of approximately 30 min, 5-hexen-1-yl *p*-toluenesulphonate (24.6 g, 96.7 mmol) was slowly added to a boiling mixture of sodium hydroxide (4.31 g, 108 mmol), 4′-hydroxy-4-bromobiphenyl (25.3 g, 102 mmol) and 300 ml of ethanol. After an additional reflux period of 8 h, the resulting white solid was filtered off and washed several times both with 200 ml of cold ethanol and 400 ml of water. After drying under vacuum at 40°C, the yield of pure 4-bromo-4′-(5-hexenyloxy)-biphenyl was 24.0 g (75%). Transitions (°C, DSC heating rate = 10°C min^{-1}): Cr 35.0 (approximately) Cr E 120.7 I.

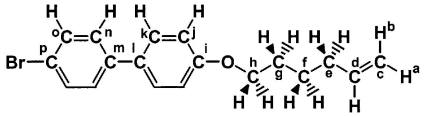

^{1}H NMR ($CDCl_3$, 25°C, 400.162 MHz): 7.52 (d, 2H, $^3J_{on} = 8.6$, H°), 7.47 (d, 2H, $^3J_{kj} = 8.8$, H^k), 7.41 (d, 2H, $^3J_{no} = 8.6$, H^n), 6.96 (2H, $^3J_{jk} = 8.8$, H^j), 5.84 (m, 1H, $^3J_{de} = 6.6$; $^3J_{db} = 17.2$; $^3J_{da} = 10.3$, H^d), 5.04 (m, 1H, $^3J_{bd} = 17.2$; $^2J = 1.4$, H^b), 4.98 (m, 1H, $^3J_{ad} = 10.3$; $^2J = 1.5$, H^a), 4.00 (t, 2H, $^3J = 6.6$, H^h), 2.14 (m, 2H, H^e), 1.83 (m, 2H, H^g), 1.59 (m, 2H, H^f). ^{13}C NMR ($CDCl_3$, 25°C, 100.630 MHz): 159.3 (C^i), 140.1 (C^m), 138.9 (C^d), 132.7 (C^l), 132.1 (C°), 128.6 (C^n), 128.3 (C^k), 121.1 (C^p), 115.2 (C^j), 115.1 (C^c), 68.2 (C^h), 33.8 (C^e), 29.1 (C^g), 25.7 (C^f).

2.3.11. *Synthesis of 4-bromo-4′-(3-butenyloxy)biphenyl (**BrE 0.4**)*

4′-Hydroxy-4-bromobiphenyl (26.2 g, 105 mmol), tetrabutylammonium bromide (525 mg, 1.63 mmol), 3-buten-1-yl *p*-toluenesulphonate (22.5 g, 99.4 mmol) and potassium carbonate (29.2 g, 211 mmol) were dissolved in 100 ml of isobutyl methyl ketone. The mixture was heated at reflux for 2 h and then cooled below 100°C, after which 80 ml of water was added. After further cooling to ambient temperature, the organic layer was separated from the aqueous layer and washed with water (250 ml), 0.1M hydrochloric acid (250 ml) and water until the pH again became neutral. Finally, the isobutyl methyl ketone was removed using a rotary evaporator. Traces of unreacted 4-hydroxy-4-bromobiphenyl, as revealed by ^{1}H NMR, were removed by washing the crude product with 0.1M sodium hydroxide (500 ml), followed by filtration and washing with water until the pH became neutral again. The yield of purified 4-bromo-4′-(3-butenyloxy)biphenyl was 24.4 g (80%). Transitions (°C, DSC heating rate = 10°C min^{-1}): Cr 51.0 S_x 123.6 I (S_x denotes an as yet unknown phase, most likely CrE).

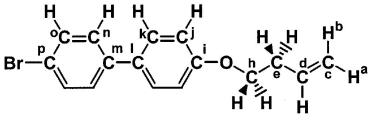

The NMR signal assignment differs from that of **BrE 0.6**, in the olefinic part. ^{1}H NMR ($CDCl_3$, 25°C, 400.162 MHz): 5.92 (m, 1H, $^3J_{de} = 6.6$; $^3J_{db} = 17.2$; $^3J_{da} = 10.2$, H^d), 5.19 (m, 1H, $^3J_{bd} = 17.2$; $^2J = 1.5$, H^b), 5.13 (m, 1H, $^3J_{ad} = 10.2$; $^2J = 1.5$, H^a), 4.06 (t, 2H, $^3J_{he} = 6.6$, H^h), 2.57 (m, 2H, $^3J_{ed} = 6.6$; $^3J_{ef} = 6.6$, H^e). ^{13}C NMR ($CDCl_3$, 25°C, 100.630 MHz): 134.7 (C^d), 117.5 (C^c), 67.7 (C^h), 34.0 (C^e).

2.3.12. *Synthesis of 4′-(5-hexenyloxy)biphenyl-4-thiol (**ThE 0.6**)*

Approximately 5 ml of a solution of 4-bromo-4′-(5-hexenyloxy)biphenyl (12.0 g, 36.2 mmol) in dry THF (150 ml) was slowly added to a mixture of dry THF (approximately 5 ml), magnesium turnings (966 mg, 39.7 mmol) and a small crystal of iodine. This mixture was carefully heated until the reaction started. The remainder of the 4-bromo-4′-(5-hexenyloxy)biphenyl/THF solution was then slowly added over a period of 2 h, while increasing the temperature to 50°C. After the addition was complete, the mixture was stirred for an additional 5 h. Small portions of approximately 250 mg of sulphur (total 1.28 g, 39.8 mmol) were then added to the solution over a one hour period. After stirring for an additional 8 h, $LiAlH_4$ (1.29 g, 34.0 mmol) in dry THF (250 ml) was carefully added to the mixture. The excess of $LiAlH_4$ was decomposed after one hour by the careful addition of water (5 ml). After filtration, drying over magnesium sulphate and subsequent evaporation, the crude product was dissolved in diethyl ether and washed with 0.1M sodium hydroxide under an argon atmosphere. The aqueous layer was added to aqueous acetic acid (0.2M), when a white precipitate was formed. Additional thiol was recovered by washing the remaining diethyl ether layer in the separation funnel several times with fresh NaOH (0.1M) until all the thiol was removed. The yield of the purified 4′-(5-hexenyloxy)biphenyl-4-thiol (**ThE 0.6**) was 2.44 g (24%). Transitions (°C, DSC heating rate = 10°C min^{-1}): Cr 85.2 CrE 111.4 I.

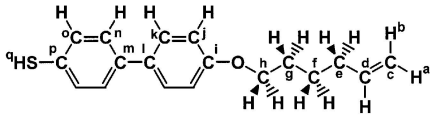

The NMR signal assignment differs from that of **BrE 0.6**, in the mercaptobiphenyl part. ^{1}H NMR ($CDCl_3$, 25°C, 400.162 MHz): 7.47 (d, 2H, $^3J_{kj} = 8.8$, H^k), 7.42 (d, 2H, $^3J_{no} = 8.4$, H^n), 7.32 (d, 2H, $^3J_{on} = 8.4$, H°), 6.95 (2H, $^3J_{jk} = 8.8$, H^j), 3.46 (s, 1H, H^q). ^{13}C NMR ($CDCl_3$, 25°C, 100.630 MHz): 159.1 (C^i), 138.8 (C^m), 133.0 (C^l), 130.3 (C°), 129.1 (C_p), 128.2 (C^k), 127.6 (C^n), 115.2 (C^j). FTIR (KBr, 20°C, cm^{-1}): 3079 (w) + 2978 (w) (C–H str. in vinyl; aryl–H str.), 2934 (m) + 2870 (m) (C–H str. in $-CH_2-$), 2554 (w) (–S–H), 1642 (m) (C=C str. in vinyl), 1607 (s) + 1524 (m) + 1485 (s) (C=C str. in aryl), 1472 (m) (C–H deform. in $-CH_2-$), 1395 (m) (C–H + CH_2 in plane def. in vinyl), 1252 (s) (C–O str. from ether funct.), 997 (w) + 912 (m) (C–H + CH_2 out of plane deform, in vinyl), 810 (s) (1,4-disubst. aryl).

2.3.13. *Synthesis of 4′-(3-butenyloxy)biphenyl-4-thiol (**ThE 0.4**)*

This compound was obtained as a white powder in 63% yield in a similar way to that for 4′-(5-hexenyloxy)biphenyl-4-thiol (**ThE 0.6**) starting from 4-bromo-4′-(3-butenyloxy)biphenyl. Transitions (°C, DSC heating rate = 10°C min^{-1}): Cr 88.5 CrE 117.8 I.

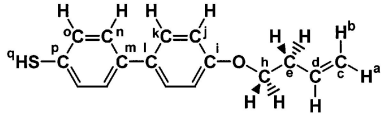

The NMR signal assignment differs from that of **BrE 0.4**, in the mercaptobiphenyl part. ^{1}H NMR ($CDCl_3$, 25°C, 400.162 MHz): 7.47 (d, 2H, $^3J_{kj} = 8.8$, H^k), 7.42 (d, 2H, $^3J_{no} = 8.4$, H^n), 7.32 (d 2H, $^3J_{on} = 8.4$, H^o), 6.95 (d, 2H, $^3J_{jk} = 8.8$, H^j), 3.46 (s, 1H, H^o). ^{13}C NMR ($CDCl_3$, 25°C, 100.630 MHz): 158.9 (C^i), 138.8 (C^m), 133.2 (C^l), 130.3 (C^o), 129.1 (C_p), 128.2 (C^k), 127.7 (C^n), 115.3 (C^j). FTIR (KBr, 20°C, cm^{-1}): 3079 (w) + 2982 (w) (C–H str. in vinyl; aryl–H str.), 2934 (m) + 2874 (m) (C–H str. in $-CH_2-$), 2554 (w) (–S–H), 1643 (m) (C=C str. in vinyl), 1607 (s) + 1524 (m) + 1485 (s) (C=C str. in aryl), 1470 (m) (C–H deform. in $-CH_2-$), 1397 (m) (C–H + CH_2 in plane def. in vinyl), 1252 (s) (C–O str. from ether funct.), 990 (m) + 916 (m) (C–H and CH_2 out of plane deform. in vinyl), 810 (s) (1,4-disubst. aryl).

3. Results and discussion

3.1. *Synthesis of phenyl benzoate derivatives*

In theory, for a substantial degree of polymerization of thiol-ene monomers to occur, an exact stoichiometric 1:1 ratio is necessary between the olefinic and thiol functionality. A possible solution to this requirement is the incorporation of both a mercapto and a vinyl group within one molecule. Several homologues of the thiol-ene **ThE *mbn*** based on a phenyl benzoate bridging unit, as shown in scheme 1, were synthesized with variations in the spacer lengths, following literature procedures when available.

The ethyl 4-(ω-bromoalkoxy)benzoate **BrA *m*** is formed by coupling an α,ω-dibromoalkane and ethyl 4-hydroxybenzoate **1**, where the ester function acts as a protective group for the carboxyl group. The desired product was separated by fractionation in vacuum from unreacted dibromide and diesters, formed from the reaction of two equivalents of **1** with the dibromide.

The primary halides thus obtained were converted to the corresponding primary thiols **ThA *m*** using thiourea. The intermediate isothiuronium salt was cleaved and the benzoic acid form was deprotected at the same time by saponification. The resulting primary mercaptan is essentially one half of the target thiol-ene monomer.

The other part of the target monomer is obtained from the reaction of hydroquinone with an alkenyl tosylate **TsE *n*** introducing the desired spacer length (scheme 1). The alkenyl tosylate is obtained using a standard procedure [16] from the commercially available ω-alkene-1-ol. The coupling of the tosylate to hydroquinone **2** can be done directly for alkenyl bromides rather than alkenyl tosylates using previously reported procedures [19–22], although significant amounts of diethers are retrieved. However, the purification is straightforward and the pure phenolic compound **PhE *n*** can be obtained in reasonable quantities. Alternatively, hydroquinone can be monoprotected, for instance using dihydropyran [18], prior to the actual coupling of the tosylate. Subsequent cleavage of the THP ether affords the phenol **PhE *n*** in better yield [7, 18].

Finally, the acid **ThA *m*** is coupled with the phenolic compound **PhE *n***, affording the final thiol-ene monomer **ThE *mbn***. This esterification was performed with the aid of dimethylaminopyridine (DMAP) and dicyclohexylcarbodiimide (DCC) in order to force the reaction to completion.

The crude products obtained from the esterifications, as reported earlier by Lub *et al.* [7], contained thioesters and disulphide contaminants as confirmed by ^{1}H NMR signals at $\delta = 3.08$, 7.92 and 2.70 ppm. An excess of the phenolic compound was used to suppress thioester formation. However, Lub *et al.* made no further attempts to purify the crude materials, as the thiol-ene monomer/thioester mixture still possessed the desired stoichiometry. Claimed efforts to purify the mixtures using column chromatography failed, due to apparent disulphide formation originating from interactions with the column materials. In this study, we successfully used flash column chromatography to separate the target thiol-ene monomer from other by-products in good yields. NMR analysis revealed that no additional disulphides or thioesters were formed when pure thiol-ene monomers were mixed with silica gel, even after heating at 60°C for several hours, a time and temperature frame that exceeds that of the actual column fractionation process. In addition, size exclusion chromatography showed no traces of molecular mass species higher than that of the monomers.

Other means of reducing the formation of by-products such as thioesters and disulphides could be the protection of the thiol functionality followed by deprotection after the final esterification to yield the target monomer [23]. However, as put forward by Lub *et al.*, the conditions for deprotection of conventional protecting groups (e.g. tetrahydropyranyl sulphanyl ether and *O*-methyl thiocarbonate) for the mercapto group resulted in the decomposition of the mesogenic core of the target monomer. We made no further efforts using different reagents for protection–deprotection, particularly since the monomer could be obtained in good yield and purity using conventional separation techniques.

3.2. *Properties of phenyl benzoate derivatives*

The synthesized thiol-ene monomers based upon the rigid phenyl benzoate core show interesting mesomorphic properties, as shown in table 1.

The thiol-ene monomers display various liquid crystalline phases as can be concluded from their typical nematic schlieren texture, and focal-conic or fan-shaped smectic A textures. The occurrence of the enantiotropic smectic A

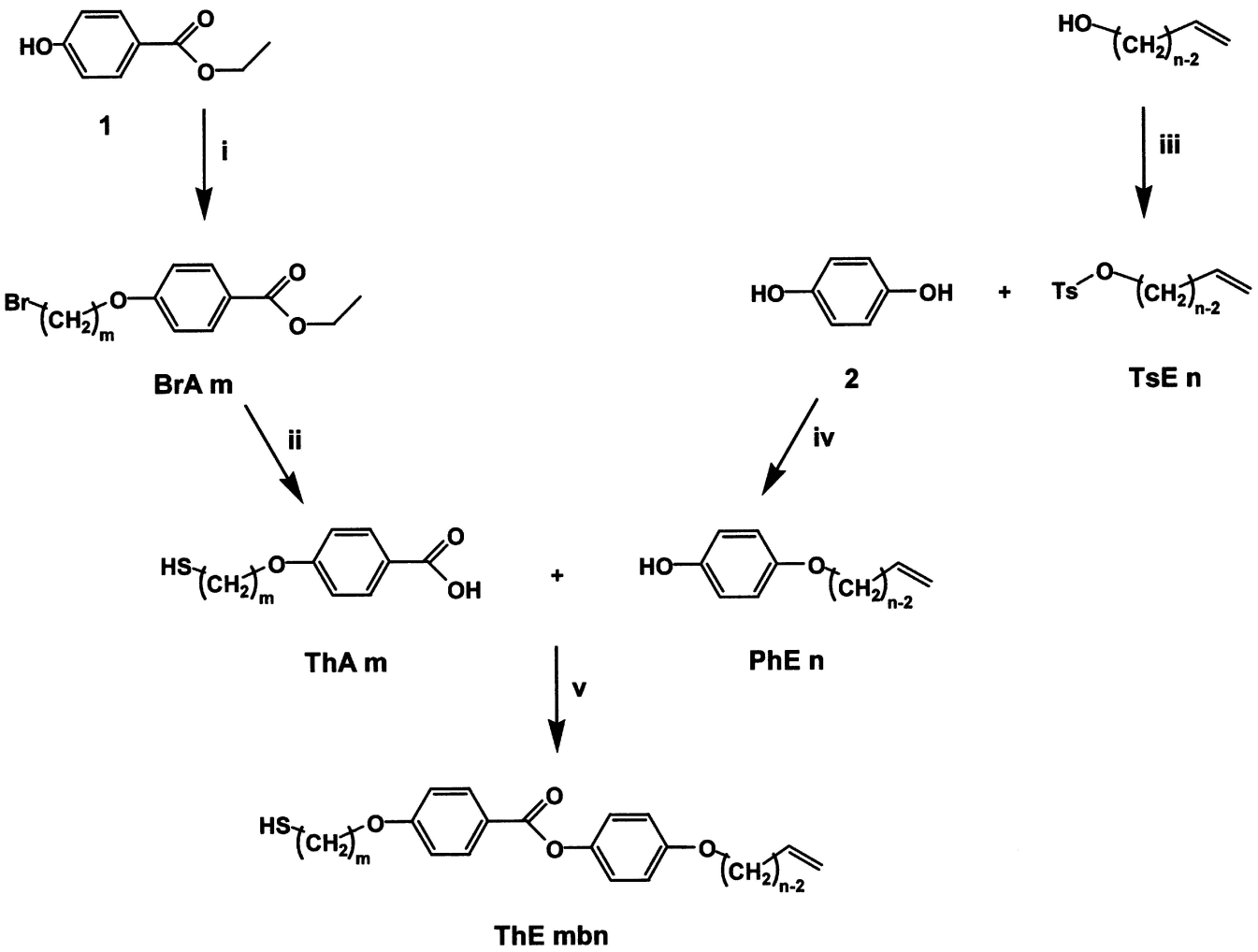

Scheme 1. Synthesis of a thiol-ene monomer containing a phenyl benzoate bridging group. The indices *m*, *n* refer to the number of carbon atoms in the spacers. The b in the acronym of the end product denotes the benzoyloxy group connecting the two phenyl rings. (i) 1. α,ω-dibromoalkane, 2. K_2CO_3; (ii) 1. thiourea, 2. NaOH; (iii) 1. pyridine, 2. TsCl; (iv) NaOH; (v) DCC/DMAP.

Table 1. Transition temperatures (°C) of the **ThE *mbn*** homologues. Cr denotes crystalline, SmA denotes smectic A, N denotes nematic and I denotes the isotropic phase. The monotropic transition is indicated in brackets. The indices *m*, *n* refers to the number of carbon atoms in the spacers.

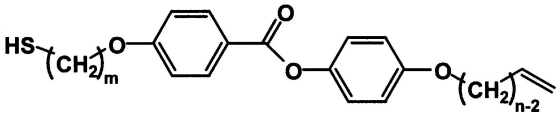

ThE mbn

Compound	*m*	*n*	Cr	→	SmA	→	N	→	I
ThE 4b4	4	4		58.6		—		68.4	
ThE 5b4	5	4		60.6		—		72.8	
ThE 6b4	6	4		53.5		(48.3)		67.7	
ThE 6b6	6	6		42.5		55.4		69.5	

phase of **ThE 6b6** and the monotropic smectic A phase of **ThE 6b4** was also confirmed by X-ray spectroscopy, see figure 1 (*a*). The corresponding layer spacings are approximately 28 and 32 Å for **ThE 6b4** and **ThE 6b6**, respectively. These values indicate a single molecule stacking within the individual layers for both monomers, as the layer spacings to a first approximation match the calculated length values obtained using minimized energy conformation calculations, 26.7 and 28.2 Å, respectively, see figure 1 (*b*).

The general transition temperatures of the thiol-ene monomers are considerably lower than those of their previously reported three-ring counterparts [7, 8] or their counterparts without thiol and vinyl groups [24]. In comparison to the three-ring thiol-enes, it is the reduced rigidity of the central mesogenic moiety that causes the nematic to isotropic transition temperature to decrease dramatically in the case of the synthesized

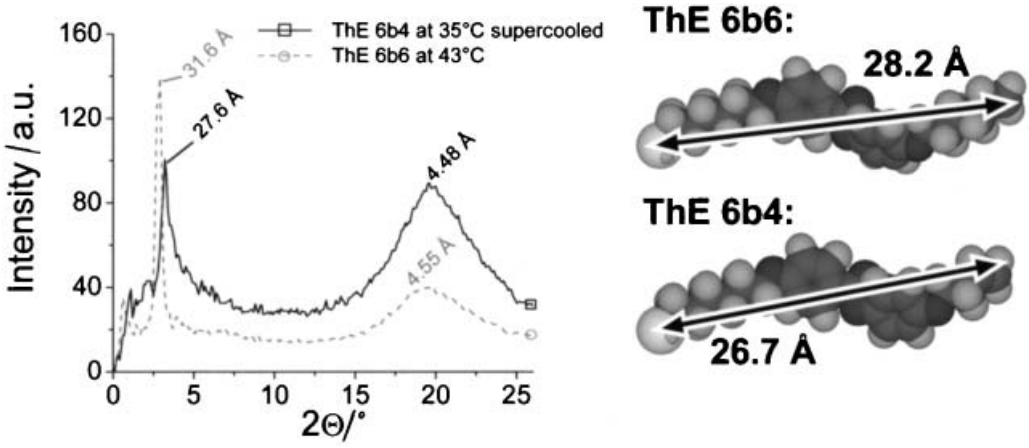

(*a*) (*b*)

Figure 1. (*a*) Diffraction curves of the smectic A phases of **ThE 6b4** and **ThE 6b6**. (*b*) Molecular models of **ThE 6b4** and **ThE 6b6** and their approximate molecular lengths.

ThE *m*b*n* monomers. In comparison with the non-substituted counterparts, mercapto and to a lesser degree olefinic functionalities also clearly contribute to the lowering of the clearing point in the case of the thiol-enes. Whereas the contribution of the olefinic group is small, or can even result in a slight increase [24, 25], the presence of the thiol group lowers the transition to a greater degree. Also, if we compare the transition temperatures reported for the incompletely purified six-spacer, two-ring thiol-ene [7], Cr 43 N 80 I, with those of the purified **ThE 6b6** (table 1), we can see that not only the clearing temperature is lower for the purified thiol-ene, but also a smectic mesophase is present. It is clear that the presence of thioester and disulphide impurities in the impure compound, with their undoubtedly higher intrinsic transition temperatures, shifts the transition temperatures of that compound upward. The stability window of the smectic phase of **ThE 6b6** is not wide enough to prevail in the binary or ternary phase diagram of the reported impure thiol-ene, consisting of the thiol-ene monomer and its contaminants.

Alternatively, it is probable that the transition temperatures of the synthesized thiol-ene homologues could be lowered even further by introducing asymmetry into the mesogenic core, for instance using a methyl substituent, as shown before for other liquid crystals [7, 26]. The use of alkyl rather than alkoxy terminal substituents also generally lowers the transition temperatures of mesogens [24]. However, these approaches may in the end result in the formation of monotropic phases or in the complete disappearance of mesophases.

From table 1 we can see that variation of the spacer length on both sides of the central core provides a versatile tool to tailor different types of reactive mesophase, ranging from the low ordered nematic to the higher ordered smectic A phase. We can also see the odd–even effect in the clearing point transitions, the highest nematic to isotropic transition occurring for the odd numbered homologue (table 1). This odd–even effect can also be found in the birefringence data for the thiol-enes shown in figure 2 (*a*). These values were obtained by polarizing optical microscopy (POM) on monolithically aligned samples using a rotary compensator.

The birefringence of the odd-spacer homologue **ThE 5b4** exceeds that of the even-spacer materials, **ThE 4b4**, **ThE 6b4** and **ThE 6b6**. The odd number of carbon atoms, together with the ether linkage and the primary thiol, facilitates packing in the mesophase and consequently results in a higher degree of order and accordingly a higher birefrigence in comparison with the even numbered homologues, where the aspect ratio is less favourable. Figure 2 (*a*) also shows the first order transition from the nematic phase to the isotropic state at the clearing point, next to the continuous transitions to the higher ordered smectic phases in the case of **ThE 6b6** and **ThE 6b4**, upon cooling. For comparison, a measurement of the birefringence of **ThE 4b4** is included, as determined by optical dichroism. Slight deviations are not unusual when comparing results from dichroism measurements and from microscopic experiments, as small deviations in the sample thickness can lead to substantial variations in the birefringence.

As the temperature dependence of the birefringence is closely related to the degree of order in a material, the order parameter can be derived from figure 2 (*a*), using the ordinary and extraordinary refractive indices of the liquid crystal, according to the extrapolation method described by Haller *et al.* [27] and Horn [28]. This is

illustrated for **ThE 6b6** in figure 2(*b*) where the refractive indices are depicted as a function of temperature. The anisotropy of the material can be observed prior to the clearing point where two refractive indices are present. The smectic to nematic transition is accompanied by a small jump in the ordinary and extraordinary refractive index. Figure 2(*c*) shows the corresponding Haller plot where T_c signifies the clearing point and $\alpha_\parallel$, $\alpha_\perp$ are the molecular polarizabilities along the molecular axis or perpendicular to it, respectively, and $\bar{\alpha}$ is the average molecular polarizability that can be calculated from the latter two values [28]. Following the local field assumption by Vuks [29], the order parameter S of a liquid crystal can be expressed as a function of the respective refractive indices by:

$$S = \left(\frac{\bar{\alpha}}{\alpha_\parallel - \alpha_\perp}\right)\frac{n_e^2 - n_o^2}{\bar{n}^2 - 1}. \qquad (1)$$

Haller observed that a linear relationship is obtained when plotting $\log[(\alpha_\parallel - \alpha_\perp)S/\bar{\alpha}]$ against the logarithmic reduced temperature, $\log(1 - T/T_c)$. The intercept (-0.5397 in this case) obtained by extrapolation to $T = 0$ K, where $S = 1$, eliminates the necessity of knowing the exact values for the individual molecular polarizabilities, as it yields the scaling factor $[(\alpha_\parallel - \alpha_\perp)/\bar{\alpha}]$ of equation (1) directly. The order parameter curve can then be constructed and is shown in figure 2(*d*) versus the reduced temperature. Again, the first order isotropic to nematic transition is visible and the order parameter climbs to a value of 0.68 for the nematic phase and further increases to 0.80 for the smectic A phase. These values are in concordance with the majority of low molecular mass calamitic liquid crystals, where maximum order parameter values can be found ranging from 0.6 to 0.8 for nematic and 0.7 to 0.9 for smectic phases. The nematic region of the order parameter curve can be

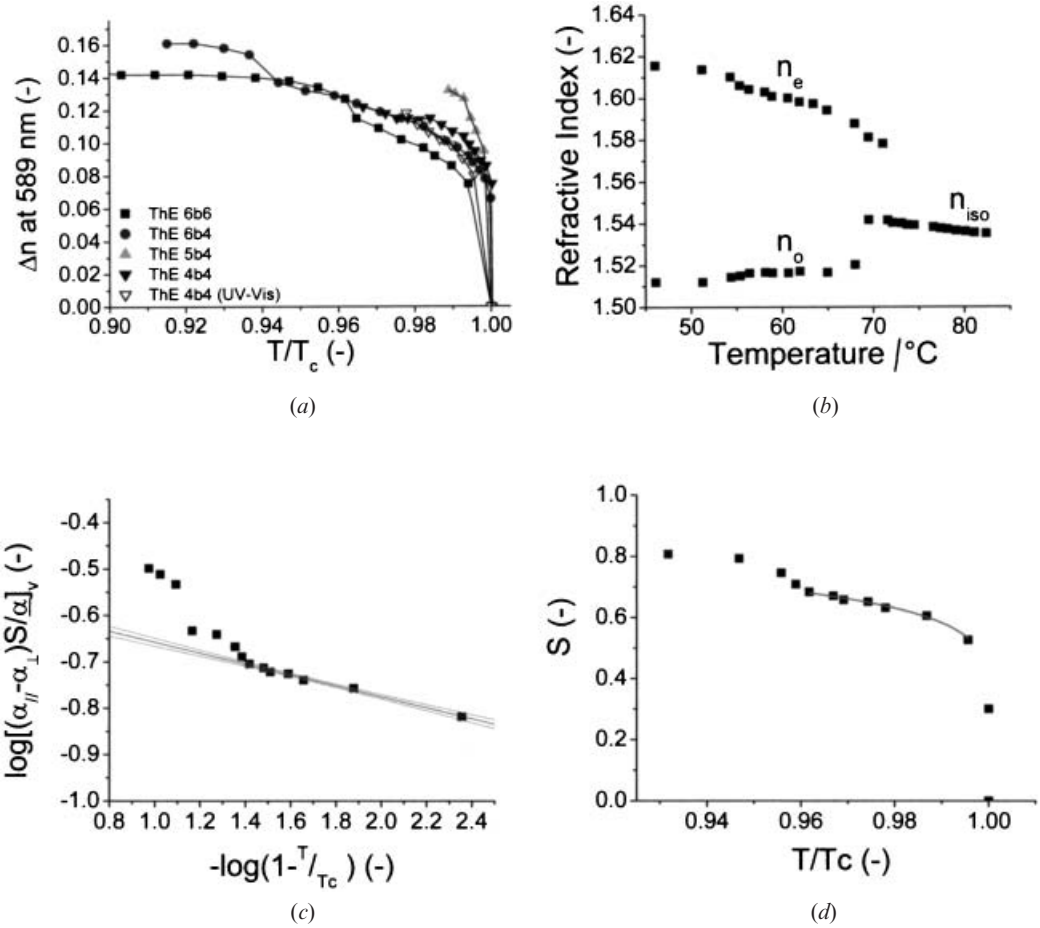

Figure 2. (*a*) Birefringence at 589 nm versus the reduced temperature for **ThE *mbn*** monomers as determined by POM using a rotary compensator; a determination by UV-Vis spectroscopy is included for comparison. (*b*) Refractive indices of **ThE 6b6** as a function of temperature. (*c*) Corresponding Haller plot showing the linear fit through the nematic region with 95% confidence limits. (*d*) Order parameter S of **ThE 6b6** versus the reduced temperature, T_c indicates the clearing point; the fit corresponds to the Maier–Saupe mean field theory for the nematic region.

adequately described using Maier–Saupe's mean field theory [30], with $S = (1 - aT/T_c)^b$, where $a = 1.00$ and $b = 0.12$.

As discussed earlier, if both the olefinic and mercapto functionalities are contained within the same monomer, this offers the benefit of an intrinsically exact stoichiometry that is required for polymerization. However, this may be realized at the expense of the intrinsic stability of the monomer, as thiol-ene polymerization can be initiated thermally and by UV-exposure. We therefore investigated the stability of the thiol-ene monomers using size exclusion chromatography (SEC) to detect the occurrence of higher molecular mass species. Figures 3(*a–c*) show the results after exposure for 15 min of **ThE 4b4**, taken as a representative for all thiol-ene monomers: to temperature alone, figure 3(*a*); temperature treatment and UV-exposure, figure 3(*b*); and exposure of the monomer and 1% w/w of photoinitiator (Irgacure 651) to UV-light at the different temperatures indicated, figure 3(*c*). We can distinguish roughly three peaks in figure 3(*a*). The large signal at a retention time of 17.3 min represents the residual monomer peak. The peaks at lower retention times reflect higher molecular mass materials such as dimeric to oligomeric species. At first glance, it appears that for those samples exposed to temperature only and to both temperature and UV-light, figures 3(*a*, *b*), hardly any polymerization occurs, as there is hardly any noticeable increase of oligomeric species. Polymerization is only noticeable for those samples that contained photoinitiator and that were irradiated at elevated temperatures, though the conversion is still low after 15 min at 70°C.

In conclusion, the liquid crystalline thiol-ene monomers synthesized are stable and odourless materials, even at elevated temperatures up to 70°C, during exposure times that exceed even typical handling times for these types of material.

3.3. *Synthesis of biphenyl derivatives*

Two homologues of the thiol-ene **ThE 0.*n*** based on a biphenyl core were synthesized with variation in the spacer lengths, as shown in scheme 2. Commercially available 4-bromo-4′-hydroxybiphenyl **3** is a suitable starting material for the synthesis of liquid crystalline thiol-ene monomers with a chemical structure that closely resembles that of cyanobiphenyls both in molecular size,

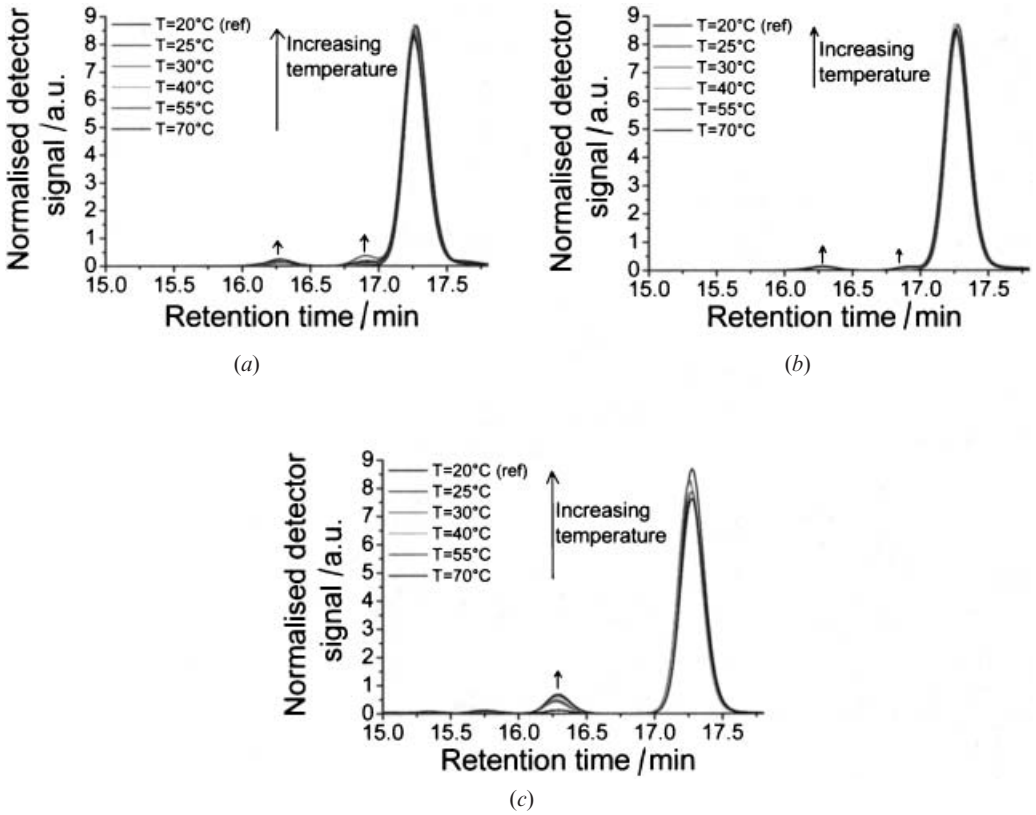

Figure 3. SEC data for **ThE 4b4** monomer exposed for 15 min to (*a*) the indicated temperatures alone, (*b*) the indicated temperatures and UV-light and (*c*) the indicated temperatures and UV-light in the presence of 1% w/w photoinitiator (Irgacure 651).

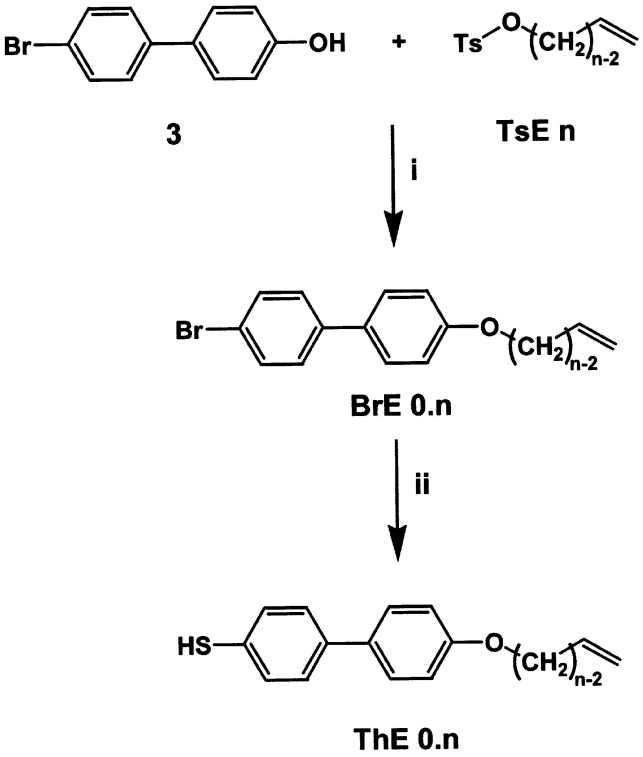

Scheme 2. Synthesis of biphenyl-based thiol-ene monomers. The index *n* refers to the number of carbon atoms in the spacers. The absence of any bridging group between the phenyl rings is denoted by a dot. (i) NaOH or K_2CO_3/$[CH_3(CH_3)_3]_4NBr$; (ii) 1. Mg (THF), 2. S, 3. $LiAlH_4$.

conformation and amphiphilic nature. Moreover, it already has two different functional groups available at the *para*-positions (4 and 4′) of the biphenyl core.

The addition of a flexible aliphatic chain containing a double bond is achieved by reaction of an alken-1-yl *p*-toluenesulphonate **TsE *n*** at the hydroxyl group of the biphenyl (scheme 2). This method was successfully used before for the phenyl benzoate-based liquid crystalline thiol-ene monomers. The reaction has to be carried out at an early stage of the synthesis sequence, before the actual thiol functionality is introduced, otherwise initially present thiol would immediately react under the alkaline conditions to form a thiolate (RS^-) ion due to the slightly acidic nature of thiols [31]. As this thiolate anion is a stronger nucleophile than the phenoxide anion, it will in turn react with the alken-1-yl *p*-toluenesulphonate. Moreover, thiolate ions can also react with atmospheric oxygen to form undesired disulfides [32].

The final step is to convert the remaining bromo substituent of the intermediate **BrE 0.*n*** into a mercapto group. The method previously used for the phenyl benzoate-based thiol-enes (i.e. conversion of a primary alkoxy halide into a primary thiol using thiourea) cannot be employed for aryl halides. Instead, the aryl halide was converted to a Grignard reagent that leads to a complex *R*–MgSBr on reaction with sulphur. The complex can be decomposed to the corresponding thiol by using hydrochloric acid [33, 34] or lithium aluminium hydride ($LiAlH_4$) [32]. The main advantage of $LiAlH_4$ over hydrochloric acid is that possible formation of disulfides is followed by their reduction to thiols when used in slight excess. Here, the Grignard synthesis with subsequent treatment by $LiAlH_4$ was successfully applied to the intermediate alken-1-yl substituted bromobiphenyls **BrE 0.*n*** to afford the biphenyl-based thiol-enes **ThE 0.*n*.**

3.4. *Properties of biphenyl derivatives*

Differential scanning calorimetry (DSC) was used to determine the phase transition temperatures of the pure monomers (**ThE 0.4** and **ThE 0.6**) and the intermediate bromobiphenyl derivatives (**BrE 0.4** and **BrE 0.6**). The results of these measurements are summarized in table 2.

The DSC onset temperatures are taken as the phase transition temperatures of the monomers and intermediate compounds. The phase transitions were also characterized using POM but it proved difficult to assess at which temperature the transition was complete. Note here that the onset temperatures listed in table 2 are measured at a rate of $10^\circ C\,min^{-1}$, and may therefore not represent the correct values due to the absence of thermodynamic equilibrium. The monomer **ThE 0.4** polymerized immediately upon heating above the Cr–CrE transition, and an accurate determination of the transition enthalpy and entropy could therefore not be accomplished. All values listed for the intermediate

Table 2. Transition temperatures (°C) of the biphenyl-based thiol-enes and the intermediate bromo compounds. Cr denotes crystalline phase, E denotes crystal E phase, I denotes isotropic phase.

Compound	Onset temperature/°C	ΔH_{tr} /kJ mol^{-1}	ΔS_{tr} /J mol^{-1} K^{-1}
BrE 0.4[a]			
Cr → E	51.0	13.3	41.2
E → I	123.6	15.8	39.8
BrE 0.6			
Cr → E	35.0	13.8	44.8
E → I	120.7	16.0	40.7
ThE 0.4			
Cr → E	88.5		
E → I	117.8		
ThE 0.6			
Cr → E	85.2	11.6	32.5
E → I	111.4	13.6	35.3

[a] Mesophase not identified unambiguously.

bromo compounds are derived from the first heating run, as no melt transition was found in the second heating run because crystallization did not occur on cooling, even after prolonged annealing.

From the onset temperatures, we can see that a decrease in spacer length results in higher transition temperatures. The decreased flexibility of the four spacer homologue apparently facilitates packing in the crystal lattice. The transition entropy corresponding to the mesophase to isotropic phase transition of **BrE 0.6** almost equals the value for **BrE 0.4**, suggesting that both bromo compounds have the same type of mesophase. Both transition entropies of **ThE 0.6** are lower than those of **BrE 0.6**. The replacement of a bromo substituent by a mercapto group apparently decreases the amount of order in both the crystalline phase and the anisotropic phase. The contribution of dimers that may be formed from the intrinsically reactive **ThE 0.6** to the increase in the degree of order is apparently small. For all compounds that are listed in table 2, all ΔS values at isotropization are considerably larger than average nematic to isotropic transition entropies with typical values in the order of 1.5–2 J mol^{-1} K^{-1} [35]. Apparently, both the thiol-ene monomers and the bromo intermediates have a highly ordered LC phase. This was confirmed by POM which revealed platelet textures that are typical for higher ordered smectic phases. Examples of these platelet textures for **BrE 0.6**, **ThE 0.6** and **ThE 0.4**, obtained upon slowly cooling from the isotropic state to a temperature of about 20°C below their isotropisation temperatures are shown in figure 4.

Wide angle X-ray scattering experiments on the pure **ThE 0.6** were performed in order to determine the nature of the liquid crystal phase. The diffraction curve, measured at 80°C (upon cooling), is illustrated in figure 5(*a*).

Three sharp outer rings are visible, which is characteristic for ordered smectic phases [36] and therefore in agreement with the smectic platelet texture observed by POM, see figure 4(*c*). X-ray diffraction calculations using Bragg's law show that the molecules are packed in an orthorhombic arrangement corresponding to a crystal E phase and the corresponding diffraction signals can be indexed accordingly. In a first approximation, minimized energy conformation calculations of the 4′-(5-hexenyloxy)biphenyl-4-thiol molecule (**ThE 0.6**) result in a calculated length, ± 18.5 Å figure 5(*b*), that equals half the layer thickness (lattice parameter *c*), as obtained from the X-ray measurements. Consequently, each layer is made up of two **ThE 0.6** molecules stacked on top of each other, see figure 5(*c*). This results in a unit cell with the lattice parameters listed in table 3.

Similar but more qualitative investigations were performed to identify the mesophases of the remaining biphenyl materials. The intermediate bromo compound **BrE 0.6** displayed a crystal E phase identical to its thiol equivalent, see figure 5(*d*). The same behaviour was observed for the monomer **ThE 0.4**, figure 5(*e*), whereas the mesophase of **BrE 0.4** could not be characterized unambiguously, being either a hexatic/crystal B phase or a crystal E phase.

Observation of crystal B or crystal E phases would be in accordance with the phases generally observed for biphenyl-type liquid crystals [24]. The majority of these materials possess single B or E type phases, or an isotropic–B–E sequence, with the strongly dipolar cyanobiphenyls as one of the few important exceptions, showing nematic and lower ordered smectic ordering.

Table 3. Lattice parameters of **ThE 0.6** at 80°C, corresponding to the orthorhombic unit cell arrangement of figure 6(*c*), determined by wide angle X-ray scattering experiments.

Lattice parameter	Measured value/Å
a	7.98
b	5.55
c	38.70

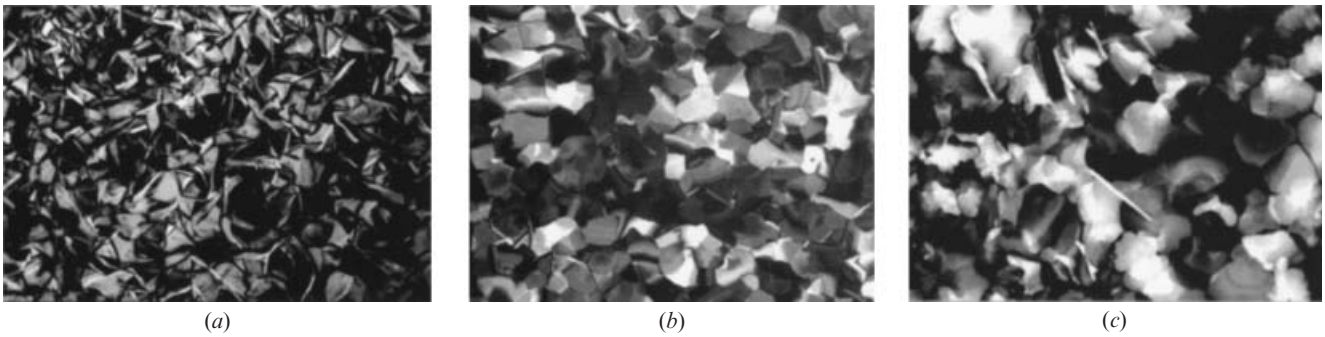

(*a*) (*b*) (*c*)

Figure 4. Texture micrographs of samples between crossed polarizers, all obtained upon cooling from the isotropic phase. (*a*) The mesophase of **ThE 0.4** at 120°C, (*b*) mesophase of **BrE 0.6** at 120°C, (*c*) mesophase of **ThE 0.6** at 95°C.

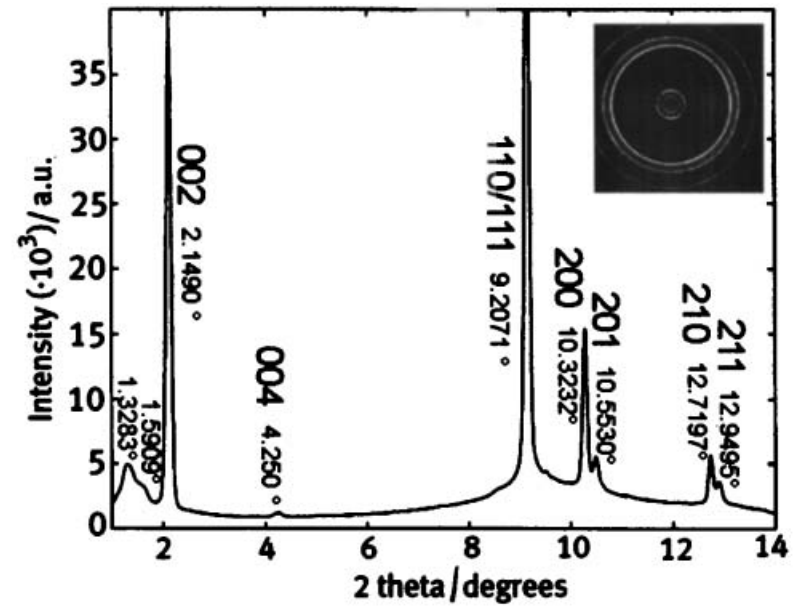

(*a*)

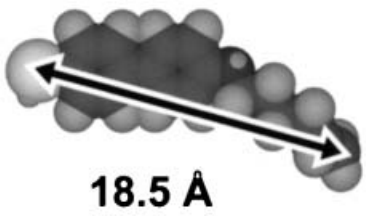

(*b*)

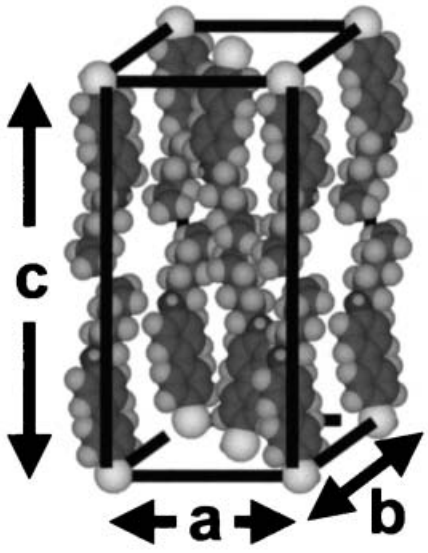

(*c*)

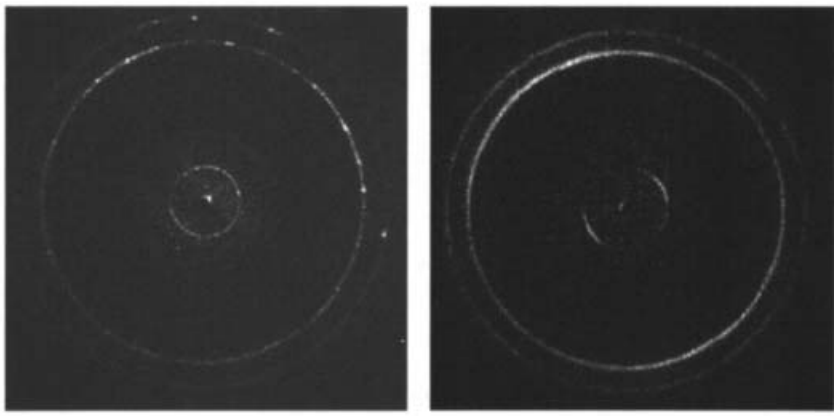

(*d*) (*e*)

Figure 5. (*a*) Wide angle X-ray scattering diffraction curve and corresponding 2D-diffraction pattern of **ThE 0.6** at 80°C, upon cooling from the isotropic phase; the reflections are indicated by their Miller indices. (*b*) Minimized energy conformation of **ThE 0.6**. (*c*) Orthorhombic unit cell arrangement corresponding to the crystal E structure of **ThE 0.6**. (*d*, *e*) 2D-diffraction pattern showing the crystal E arrangements of **BrE 0.6** and **ThE 0.4**, respectively.

3.5. *Mixing behaviour of biphenyl derivatives*

In order to polymerize these thiol-ene monomers from an anisotropic solvent, it is obviously necessary for the monomers initially to form one homogeneous liquid crystalline phase with the cyanobiphenyl solvents used. This is analogous to the situation described for phenyl benzoate-based thiol-enes [37]. Unfortunately, the odds on the successful formation of a homogeneous liquid crystalline phase when mixing highly ordered smectic phases and nematic mesogens are in general not very high [36]. Nevertheless, from a thermodynamic standpoint a region could exist where a homogeneous nematic

phase exists for low monomer concentrations in the anisotropic solvent. Figure 6 depicts preliminary results regarding the mixing behaviour of the liquid crystalline thiol-ene monomer **ThE 0.6** with the cyanobiphenyl **6CB**, as determined by DSC, optical microscopy and X-ray spectroscopy. Note that the binary phase diagram is not completed for high monomer concentrations and that the positions of most lines in the phase diagram are estimations based on the measured transitions, and may therefore not correspond to the real positions.

Extensive two-phase regions are present in the binary phase diagram showing the anticipated difference between the molecular order of the monomer and the solvent. In addition, the large gap between the transition temperatures of both components certainly contributes to the non-mixing behaviour. In any case, a homogeneous nematic phase is experimentally not accessible. Similar results were found for **ThE 0.4**/**6CB** and **ThE 0.4**/**E7** combinations [17], thus eliminating these monomer/solvent combinations for practical use. With respect to the *in situ* polymerizations of these biphenyl-based thiol-ene monomers in anisotropic solvents, either different solvents are required or chemical modification of the monomers may be considered to enhance the solubility in the cyanobiphenyl solvents, such as the introduction of small lateral substituents.

However, the biphenyl-based thiol-ene monomers introduced here display a high intrinsic molecular degree of order and therefore form interesting reactive materials for the creation of main chain polymers with highly defined mechanical and optical or electro-optical properties. Future investigations will consequently be directed to the bulk polymerization behaviour of these monomers and the evaluation of their properties in bulk, in self-assembly processes and in (polymerizable free-standing) thin films with a high degree of order.

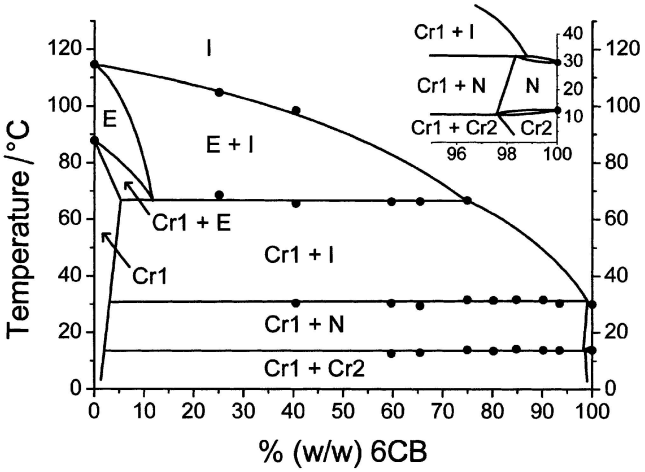

Figure 6. Binary phase diagram of **ThE 0.6** and **6CB**. The inset shows a magnification of the region low in monomer. Cr ('1' denotes **ThE 0.6**, '2' denotes **6CB**), E, N and I denote the crystalline, crystal E, nematic and isotropic phases, respectively.

4. Conclusions

In this work, we have synthesized novel phenyl benzoate-based and biphenyl-based liquid crystalline thiol-ene monomers. The synthesis of these odourless monomers proved to be straightforward, and can easily be adapted to create further homologues. The type of mesophase can be tuned from the low ordered nematic and smectic A phase to highly ordered mesophases, e.g. crystal E phase, by the appropriate choice of bridging group and variation of the spacer lengths. Stability issues resulting from a 1:1 thiol-olefin ratio, possibly leading to premature polymerization of the low melting phenyl benzoate-based thiol-enes, are not a major concern, especially at typical handling temperatures and times. Their remarkably low transition temperatures, stability and variable mesophases make the phenyl benzoate-based liquid crystalline monomers particularly interesting for establishing reactive mixtures with inert isotropic and anisotropic solvents. The subsequent polymerization of these monomers, whether performed in bulk or *in situ*, will lead to novel main chain liquid crystalline thiol-ene polymers and polymer architectures, completely different from those based on side group liquid crystalline polymers or network-type structures. Consequently, the phenyl benzoate-based thiol-ene monomers could ultimately form the basis of completely new types of liquid crystal-based devices with enhanced electro-optical properties.

Although the use of the biphenyl-based thiol-ene monomers appears to be of limited use for polymerizations in cyanobiphenyl solvents, variation of the anisotropic solvent or chemical modification of the monomer by lateral substituents, for instance, could resolve this. The synthesized biphenyl-based thiol-ene monomers form a particularly interesting class of reactive materials that can be bulk polymerized to give main chain polymers with highly defined mechanical and optical or electro-optical properties resulting from the intrinsic high molecular order of the corresponding monomers.

References

[1] Fergason, J. L., 1985, *SID Dig. Tech. Pap.*, **16,** 68.
[2] Van Boxtel, M. C. W., Janssen, R. H. C., Broer, D. J., Wilderbeek, H. T. A., and Bastiaansen, C. W. M., 2000, *Adv. Mater.*, **12,** 753.
[3] Coles, H. J., 1985, *J. chem. Soc. Faraday Discuss.*, **79,** 201.
[4] Drzaic, P. S., 1995, *Liquid Crystal Dispersions* (Singapore: World Scientific).
[5] Hikmet, R. A. M., 1990, *J. appl. Phys.*, **68,** 4406.

[6] Wilderbeek, H., de Koning, H., Vorstenbosch, J., Chlon, C., Bastiaansen, C. W. M., and Broer, D. J., 2002, *Jpn. J. appl. Phys., 1*, **41,** 2128.
[7] Lub, J., Broer, D. J., and van den Broek, N., 1997, *Liebigs Ann./Recueil*, 2281.
[8] Lub, J., Broer, D. J., Martinez Antonio, M. E., and Mol. G. N., 1997, *Liq. Cryst*., **24,** 375.
[9] Fukumasa, M., Takeuchi, K., and Kato, T., 1998, *Liq. Cryst*., **24,** 325.
[10] Kato, T., Kutsuna, T., Hanabusa, K., and Ukon, M., 1998, *Adv. Mater*., **10,** 606.
[11] Mizoshita, N., Kutsuna, T., Hanabusa, K., and Kato, T., 1999, *Chem. Commun*., **9,** 781.
[12] Jacobine, A. F., 1993, *Radiation Curing in Polymer Science and Technology*, edited by J. P. Fouassier and J. F. Rabek (London: Elsevier Applied Science), pp. 219–268.
[13] Wilderbeek, H. T. A., van der Meer, F. J. A., Feldman, K., Broer, D. J., and Bastiaansen, C. W. M., 2002, *Adv. Mater*., **14,** 655.
[14] Vogel, A. I., 1989, *Vogel's Textbook of Practical Organic Chemistry* (Singapore: Longman).
[15] Höhne, G. W. H., Hemminger, W., and Flammersheim, H.-J., 1996, *Differential Scanning Calorimetry: an Introduction for Practitioners* (Berlin: Springer-Verlag).
[16] Chabrand, C. J., McNally, J. P., and Little, I. R., 1994, EP 586 167 A1.
[17] Wilderbeek, H., 2001, PhD thesis, Eindhoven University of Technology, The Netherlands, ISBN 90-386-2972-9.
[18] Jahromi, S., Lub, J., and Mol, G. N., 1994, *Polymer*, **35,** 622.
[19] Kelly, S. M., Buchecker, R., and Schadt, M., 1988, *Liq. Cryst*., **3,** 1115.
[20] Broer, D. J., Lub, J., and Mol, G. N., 1993, *Macromolecules*, **26,** 1244.
[21] Schnurpfeil, G., Harder, A., Schröder, H., Wöhrle, D., Hartwig, A., and Hennemann, O.-D., 2001, *Macromol. Chem. Phys*., **202,** 180.
[22] Marty, J.-D., Mauzac, M., Fournier, C., Rico-Lattes, I., and Lattes, A., 2002, *Liq. Cryst*., **29,** 529.
[23] Greene, T. W., and Wuts, P. G. M., 1991, *Protective Groups in Organic Synthesis* (New York: Wiley-Interscience).
[24] Vill, V., 1992, Group IV, Vols. 7a and b, in *Landolt-Börnstein, New Series*, edited by J. Thiem (Berlin: Springer-Verlag).
[25] Krücke, B., Schlossarek, M., and Zaschke, H., 1988, *Acta Polym*., **39,** 607.
[26] Broer, D. J., 1993, *Radiation Curing in Polymer Science and Technology*, edited by J. P. Fouassier and J. F. Rabek (London: Elsevier Applied Science), pp. 383–443.
[27] Haller, I., Huggins, H. A., Lilienthal, H. R., and McGuire, T. R., 1973, *J. phys. Chem*., **77,** 950.
[28] Horn, R. G., 1978, *J. Phys. (Les Ulis, Fr.)*, **39,** 105.
[29] Vuks, M. F., 1996, *Opt. Spectrosk*., **21,** 697.
[30] Maier, W., and Saupe, A., 1958, *Z. Naturforsch*., **13a,** 564.
[31] Crampton, M. R., 1974, *The Chemistry of the Thiol Group*, edited by S. Patai (London: John Wiley), pp. 379–416.
[32] Smith, M. B., and March, J., 2001, *March's Advanced Organic Chemistry. Reactions, Mechanisms, and Structure* (New York: Wiley-Interscience).
[33] Szmuszkovicz, J., 1969, *Org. Prep. Proced*., **1,** 43.
[34] Šindelár, K., Metyšová, J., and Protiva, M., 1972, *Collect. Czech. chem. Commun*., **37,** 1734.
[35] Vertogen, G., and de Jeu, W. H., 1988, *Thermotropic Liquid Crystals, Fundamentals* (Berlin: Springer-Verlag).
[36] Gray, G. W., and Goodby, J. W. G., 1984, *Smectic Liquid Crystals* (Glasgow: Leonard Hill).
[37] Wilderbeek, H. T. A., van der Meer, M. G. M., Bastiaansen, C. W. M., and Broer, D. J., 2002, *J. Phys. Chem. B* (accepted).